Published in final edited form as:
Circ Res. 2009 September 25; 105(7): 648–656. doi:10.1161/CIRCRESAHA.109.203109.

iPS Programmed Without c-MYC Yield Proficient Cardiogenesis for Functional Heart Chimerism

Almudena Martinez-Fernandez, **Timothy J. Nelson**, **Satsuki Yamada**, **Santiago Reyes**, **Alexey E. Alekseev**, **Carmen Perez-Terzic**, **Yasuhiro Ikeda**, and **Andre Terzic***
Marriott Heart Disease Research Program, Division of Cardiovascular Diseases, Departments of Medicine, Molecular Pharmacology and Experimental Therapeutics, and Medical Genetics, Mayo Clinic, Rochester, MN (A.M.F., T.J.N., S.Y., S.R., A.E.A., C.P.T., A.T.); Department of Physical Medicine and Rehabilitation, Mayo Clinic, Rochester, MN (C.P.T.); Department of Molecular Medicine (Y.I.), Mayo Clinic, Rochester, MN

Abstract

Rationale—Induced pluripotent stem cells (iPS) allow derivation of pluripotent progenitors from somatic sources. Originally, iPS were induced by a stemness-related gene set that included the c-MYC oncogene.

Objective—Here, we determined from embryo to adult the cardiogenic proficiency of iPS programmed without c-MYC, a cardiogenicity-associated transcription factor.

Methods and Results—Transgenic expression of three human stemness factors SOX2, OCT4, and KLF4 here reset murine fibroblasts to the pluripotent ground state. Transduction without c-MYC reversed cellular ultrastructure into a primitive archetype and induced stem cell markers generating three-germ layers, all qualifiers of acquired pluripotency. Three-factor induced iPS (3F-iPS) clones reproducibly demonstrated cardiac differentiation properties characterized by vigorous beating activity of embryoid bodies and robust expression of cardiac Mef2c, alpha-actinin, connexin43, MLC2a, and troponin I. In vitro isolated iPS-derived cardiomyocytes demonstrated functional excitation-contraction coupling. Chimerism with 3F-iPS derived by morula-stage diploid aggregation was sustained during prenatal heart organogenesis, and contributed in vivo to normal cardiac structure and overall performance in adult tumor-free offspring.

Conclusions—Thus, 3F-iPS bioengineered without c-MYC achieve highest stringency criteria for bona fide cardiogenesis enabling reprogrammed fibroblasts to yield de novo heart tissue compatible with native counterpart throughout embryologic development and into adulthood.

Keywords

induced pluripotent stem cells; chimera; cardiac; nuclear reprogramming

Induced pluripotent stem cell (iPS) technology offers a promising approach to produce unlimited supplies of replacement tissues from autologous sources.[1–3] Ectopic transgene expression with a set of four stemness factors OCT3/4, SOX2, KLF4, and c-MYC has proven adequate to reprogram somatic cell nuclei, inducing a pluripotent ground state.4 By demonstrating reversibility of cell fate through coerced reprogramming of gene expression,

*Correspondence to Andre Terzic, MD, PhD, Mayo Clinic, 200 First Street SW, Rochester, MN 55905; Fax: (507) 266-9936; Phone: (507) 284-2747; terzic.andre@mayo.edu.

Disclosures None

this robust platform has unmasked the atavistic potential of ordinary cells [5–9] and the gain of regenerative aptitude.[10–12] Progeny that acquires a stem cell-like capacity with spontaneous and efficient differentiation, a quality reserved for embryonic stem cells, has produced diverse cytotypes including authentic cardiac myocytes.[13–17]

With the prospect of obtaining bioengineered heart tissue from somatic sources, validated iPS create unprecedented opportunities for disease-specific model systems, tailored drug discovery, and individualized regenerative therapeutics.[17–19] To this end, iPS technology must reproducibly generate functional lineage-specific tissues without provoking long-term dysregulated cell growth. Nuclear reprogramming was originally identified according to the transgene expression of stemness-related gene foursomes that included oncogenes such as, c-Myc, to de-differentiate the cell and acquire pluripotent features. Multiple strategies are employed to reduce oncogenic load, including non-integrating systems to prevent deleterious genomic modifications.[20–24] Eliminating proto-oncogenes during reprogramming effectively decreases the risk of tumorigenic transformation within offspring.[25] However, analysis of stem cell-like pools produced with alternative gene sets has focused on criteria of functional pluripotency,[26] without delineating the impact on cardiac-specific differentiation.

Cardiogenicity of murine and human iPS cells, reprogrammed utilizing c-Myc or an equivalent Lin28, is consistent with cardiac differentiation established with native embryonic stem cells.[13–17] In fact, c-Myc-dependent pathways are documented in the induction of the cardiac fetal gene expression profile,[27] and expression in transgenic hearts activates adaptive stress response provoking cell cycle re-entry.[28] Although c-Myc is linked to cardiovascular gene expression,[27–29] it is unknown how removal of this transcription factor would affect reprogrammed iPS to reproducibly generate cardiac tissue. Tissue-specific differentiation from iPS and proper integration into host tissue are metrics that must be met to ensure usefulness of the reprogramming technology.[30] Thus it is warranted to determine iPS-based cardiac lineage derivation independent of the c-Myc transgene, and probe the multi-dimensional process of development needed for functional cardiogenesis.

In the absence of c-MYC, nuclear reprogramming of ordinary fibroblasts with three human stemness-related factors OCT3/4, SOX2, and KLF4 generated pluripotent progeny (3F-iPS). The acquired cardiogenicity enabled formation of *de novo* tissue with initiation of force-generating electro-mechanical coupling that functioned according to stage-specific cardiac progenitors. Proficient cardiac lineage from 3F-iPS created synchronized cardiogenesis within the developing embryo and throughout adult chimera.

Materials and Methods

Fibroblast transduction

Mouse embryonic fibroblasts (MEF), plated in Dulbecco's modified Eagle's medium with 10% FCS, 1% L-glutamine and penicillin/streptomycin (Invitrogen) at 10^5 per 24-well plate, were infected for 12 h with full-length human OCT3/4, SOX2 and KLF4 cDNAs (Open Biosystems) using a lentivirus system.31 The rationale for using human genes for reprogramming was to determine whether human cDNA is phylogenetically conserved to produce iPS with cardiogenic potential. MEF were maintained in Dulbecco's modified Eagle's medium supplemented with pyruvate (Lonza) and L-glutamine, non-essential amino acids (Mediatech), 2-mercaptoethanol (Sigma-Aldrich), 15% FCS and LIF (Millipore). Within 3 weeks, iPS clones were isolated and labeled with LacZ and luciferase using pLenti6/UbC/V5-GW/LacZ (Invitrogen) and a pSIN-Luc luciferase-expressing vector.31 Vector integration was PCR confirmed from genomic DNA (Sigma-Aldrich, XNAT2) using primers for OCT4-R AGCCGCCTTGGGGCACTAGCCC, KLF4-R

CGCAAGCCGCACCGGCTCCGCC, SOX2-R AGCCTCGTCGATGAACGGCCGC, and SFFVprom-F CTCACTCGGCGCGCCAGTCCTC. PCR products were resolved on 1% agarose gel electrophoresis.

Cell sorting and electron microscopy

LacZ labeled clonal populations were trypsinized, incubated with Fluorescein di[β-D-galactopyranoside] (Sigma-Aldrich, F2756),[32] and sorted using a FACS Aria SE flow cytometer (BD Biosciences). On fixation with 1% glutaraldehyde and 4% formaldehyde in 0.1 M phosphate buffered saline (pH 7.2), cells were examined on a Hitachi 4700 field emission scanning microscope.33 For ultrastructural evaluation, fixed cells were ultramicrotome cut, and stained with lead citrate prior to examination on a JEOL 1200 EXII electron microscope.34

Immunostaining and confocal microscopy

Cells were stained with anti-SSEA1 antibody (MAB4301; dilution 1:50; Millipore) along with secondary goat anti-mouse IgG Alexa Fluor 568 (Sigma A11031; 1:250) or alkaline phosphatase detection kit (Millipore, SCR004). Immunostaining of derivatives was performed using monoclonal mouse anti-alpha-actinin (Sigma A7811, 1:200), rabbit anti-connexin 43 (Zymed 483000, 1:200), rabbit anti-Mef2c (proteintech 10056-1-AP, 1:50) and monoclonal mouse anti-myosin light chain 2a (MLC2a, Synaptic Systems 311011, 1:250), Cardiac Troponin I (Abcam 47003, 1:500). Secondary antibodies (Invitrogen) were used at a 1:250 dilution (i.e. goat anti-mouse IgG Alexa Fluor 568, donkey anti-mouse IgG Alexa Fluor 488 and goat anti-rabbit IgG Alexa Fluor 488). Nuclei were labeled with 4,6'-diamidino-2-phenylindole (DAPI; Invitrogen). Images were taken using laser confocal microscopy (Zeiss LSM 510 Axiovert). For LacZ staining, samples were fixed with 0.25% gluteraldehyde for 15 min at room temperature prior to β-galactosidase staining.

In vivo and *in vitro* differentiation

Transduced fibroblasts were injected subcutaneously into the flank skin of anesthetized athymic nude mice or immunocompetent C57BL/6 strain of mice at 500,000/50 μl medium. Local growth was monitored daily until tissue was harvested and processed by rapid freezing, and cryosectioned for hematoxylin/eosin procedures. Separately, iPS were differentiated into three-layer embryoid bodies (EB) using the hanging-drop method.35,36 Digital serial images were analyzed with Metamorph (Visitron Universal Imaging).

Gene expression

Expression of pluripotent, gastrulation, and cardiac markers was detected by RT-PCR.[37,38] Mouse *Gapdh* (4352932E; Applied Biosystems) was used as control. Analyzed genes included *Sox2* (Mm00488369_s1), *Oct4* (Mm00658129_gH), *Fgf4* (Mm00438917_m1), *Gsc* (Mm00650681_g1), *Sox17* (Mm00488363_m1), *Mesp2* (Mm00655937_m1), *Tbx5* (Mm00803521_m1), *Nkx2*.5 (Mm00657783_m1) and *Mef2c* (Mm01340839_m1; Applied Biosystems).

Patch clamp and calcium imaging

Derived cardiomyocytes, enriched by dual interface Percoll gradient (Invitrogen),[39] were plated on laminin coated coverglass for >24 h. Membrane electrical activity was determined by patch-clamp recording in the whole cell configuration using current- or voltage-clamp mode (Axopatch 1C, Axon Instruments). Action potential profiles and voltage-current relations were acquired and analyzed with the Bioquest software. Cells were superfused with Tyrode solution containing (in mM) 137 NaCl, 5.4 KCl, 2 $CaCl_2$, 1 $MgCl_2$, 10 HEPES, and 10 glucose (with pH adjusted to 7.3 with NaOH) or calcium-free Tyrode in which $CaCl_2$

was replaced by EGTA 5 mM. Patch pipettes (5–10 MΩ) containing (in mM) 140 KCl, 1 $MgCl_2$, 10 HEPES, 5 EGTA, and supplemented with 5 mM ATP (with pH adjusted to 7.3 with KOH) were used for electrophysiological measurements performed at 34±1°C set by a Peltier thermocouple temperature controller. To assess intracellular Ca^{2+} dynamics, cells were loaded with the Ca^{2+}-fluorescent probe Fluo 4-AM (Invitrogen), imaged with a Zeiss LSM live 5 laser confocal microscope, and analyzed using LSM software.[39]

Chimeric blastocyst formation and *in utero* organogenesis

CD1 embryos were harvested at 2.5 days post coitum (dpc) and plated as pairs in microwells for diploid aggregation.17,40 LacZ-labelled cells cultured for at least two passages after thawing were partially digested using trypsin 0.25%-EDTA and pre-plated for 45 min to allow attachment of feeders. Floating clumps (8–15 cells) were co-incubated with embryo pairs in microwells. The aggregation complex was incubated for 24 h until cavitation of blastocysts.17,40 Surrogate mothers were anesthetized (2–3% inhaled isoflurane), uterus dissected through a minimal flank incision, and blastocyst-stage chimeric aggregates transferred into the uterus.40 Pseudopregnant females supported pregnancy until days 8.0–9.5 dpc, when embryos were harvested and analyzed for LacZ-labelled progenitors using a ProgRes C3 camera-equiped Zeiss stereo Discovery V20 microscope. Embryos were fixed with 0.25% gluteraldehyde for 15 min at room temperature prior to β-galactosidase staining.

Molecular imaging

Luciferase-transfected iPS were cultured for multiple passages including a freeze/thaw cycle prior to expansion and transplantation into recipients. Cells were tracked with the IVIS 200 Bioluminescence Imaging System (Xenogen) following intra-peritoneal injection of 150 mg/kg D-luciferin (Xenogen), and signals analyzed with the Living Image Software (Xenogen).[17]

Electrocardiography and echocardiography

In age-matched control and iPS-chimera mice under anesthesia (1.5% isoflurane), heart rate and rhythm were measured using 4-limb lead electrocardiography (MP150, Biopac). Cardiac structure, and left ventricular contractility were quantified by transthoracic echocardiography using a 30 MHz MS400 transducer (Vevo2100, Visual Sonics).[41]

Statistics

Data are presented as mean±SEM. Student's t test was used to evaluate significance of PCR data. Wilcoxon test was used to evaluate physiological parameters between chimeric and non-chimeric cohorts. A p value <0.05 was predetermined.

RESULTS

Phylogenetically conserved nuclear reprogramming with human stemness factors independent of c-MYC

MEFs grown in monolayers demonstrated contact inhibition upon culture confluency. Elongated flat cells typical of fibroblasts provided a homogenous population of starting somatic tissue (Figure 1A). Upon cross-species transduction with three human stemness-related factors, SOX2, OCT4, and KLF4, vector-derived transgenes were stably integrated in engineered progeny, absent from the untransduced parental source (Figure 1A). Scanning electron microscopy documented structural metamorphosis, revealing isolated colonies that exhibited a condensed morphology in contrast to the flat untransduced neighboring fibroblasts (Figure 1B, left side). Transmission electron microscopy imaged a reduced cytosol-to-nuclear ratio in transduced progeny, indicating acquisition of primitive cell

phenotype (Figure 1B, right side). Tightly packed colonies, which represent clonal clusters of reprogrammed cells, robustly expressed markers of pluripotency, alkaline phosphatase (AP; left side) and SSEA-1 (right side), negligible in parental fibroblasts (Figure 1C). To validate acquired pluripotency *in vivo*, cells transduced with three human stemness factors (3F-iPS) were injected subcutaneously into immunodeficient mice. Within weeks following delivery of 500,000 3F-iPS, three germ layers were detected on histology, including glandular epithelium (endoderm), keratinized epidermal ectoderm (ectoderm) and mesenchymal derived connective tissue (mesoderm; Figure 2A). Molecular analysis identified cardiac tissue that demonstrated sarcomeric striations (Figure 2B, left), and typical markers such as alpha-actinin (Figure 2B, middle), cardiac troponin I and sarcolemmal connexin 43 (Figure 2B, right). Thus human transcription factors SOX2, OCT4, and KLF4, in the absence of c-MYC, induced phylogenetic nuclear reprogramming from murine fibroblasts to achieve functional pluripotency across species.

Three factor iPS-derived embryoid bodies unmask reproducible cardiogenic potential

Distinct 3F-iPS clones consistently yielded clusters of undifferentiated cells capable of generating embryoid spheroids at day 5 following a hanging-drop protocol, and differentiated in three-dimensional cultures throughout a 12-day period (Figure 3A). iPS progeny were sampled sequentially starting at day 0 monolayers (Figure 3A, top), day 5 floating embryoid spheres (Figure 3A, middle), and day 12 plated embryoid bodies (Figure 3A, bottom). Gene expression analysis from two independent clones, sampled throughout the continuum of differentiation, demonstrated immediate, sustained, and reproducible downregulation of pluripotent markers Oct4, Sox2, and Fgf4 (Figure 3B; $p<0.05$). Recapitulating gastrulation in the embryo, induction of mesoderm (Goosecoid, Gsc) and endoderm (Sox17) peaked by day 5 in iPS-derived embryoid bodies, giving rise to the pre-cardiac mesoderm identified by Mesp2 expression (Figure 3C; $p<0.05$). Cardiac differentiation was further indicated by a 20–30 fold upregulation in cardiac transcription factors Tbx5, Nkx2.5, and Mef2c by day 12, compared to undifferentiated day 0 iPS (Figure 3D; $p<0.05$). Thus, the pattern of gene expression in 3F-iPS, verified across all tested clones, revealed exchange of genes with pluripotent potential for the acquired proficiency of lineage specification, ensuring reproducible cardiogenic outcome.

Functional cardiogenesis derived from 3F-iPS

iPS differentiating within embryoid bodies (EB) were examined daily to quantify the percentage of EB that acquired cardiac phenotype tracked by spontaneous beating activity. Independent clones derived by three-factor reprogramming revealed consistent progression of beating activity as early as 7 days following progeny differentiation (Figure 4A) that corresponded to expression of cardiac contractile proteins (Figure 4A, inset). From ~10% of contracting EB within independent clones starting two days after plating EB at day 5, the percentage of beating areas progressively increased through day 11 with 54–72% of all colonies containing at least one area of spontaneous contractions (Figure 4A). Notably, EB that demonstrated multiple beating areas (Figure 4B top, rectangles) developed synchronized contractile rhythm underlying coordinated electrical activity that propagated through the syncytium of nascent cardiac tissue (Figure 4B bottom). Isolation of cardiomyocytes from beating EB was achieved using a selective density gradient. Structural changes consistent with cardiac differentiation were observed at day 12 as 3F-iPS progeny developed rod-shaped morphology (Figure 4C, top), a mature myofibrillar organization (Figure 4C, middle), and gap junctions that bridged adjacent progeny (Figure 4C, bottom). Similarly, iPS-derived cells demonstrated presence of the cardiac transcription factor Mef2c, contractile protein alpha actinin, and gap junction-protein connexin 43 (Figure 4D). Moreover, spontaneous action potential activity was recorded in isolated cells under whole cell current-clamp mode (Figure 4E). Under voltage-clamp, depolarization of 3F-iPS

progeny by membrane potentials imposed ramp pulses from −100 to +60 mV revealed prominent inward and outward current components, not present in non-excitable parental fibroblasts (Figure 5A). The inward current component was eliminated in the absence of external Ca^{2+} (Figure 5B). Furthermore, removal of Ca^{2+} reversibly abolished action potential activity in 3F-iPS derived cardiac cells (Figure 5C). Loaded with the calcium selective Fluro-4AM probe, 3F-iPS derived cardiomyocytes demonstrated rhythmic transients consistent with calcium dynamics in diastole versus systole (Figure 5D), in synchrony with force-generating mechanical contractions (Figure 5E). These data indicated reproducible derivation of 3F-iPS progeny that progressively acquired authentic cardiogenic machinery required for excitation-contraction coupling, and generation of functional cardiomyocytes.

3F-iPS chimerism contributes to *de novo* heart tissue formation in the embryo and sustains cardiac function in the adult heart

Non-coerced diploid aggregation at the morula stage allows competent pluripotent stem cells to assimilate within a developing embryo and contribute to chimeric organogenesis.[17,40] 3F-iPS labeled with LacZ and luciferase expression cassettes were clonally expanded and allowed aggregation with two, 8-cell morula embryos (Figure 6A and 6B). The process of diploid aggregation, that engages equivalent progenitors into a chimeric blastocyst, exploited the ability of 3F-iPS to integrate into host embryos and function as a blastomere, demonstrated by mosaic distribution of positive lacZ-expressing iPS progeny (Figure 6C and 6D). iPS-derived tissue populated the embryo (n=7) during development and contributed to all stages of cardiogenesis from primitive heart fields to looped heart tubes corresponding to 8.0 to 9.5 dpc, respectively (Figures 6E–6G). By 9.5 dpc when the heart tube has fully looped to form distinct inflow and outflow tracts, iPS progeny was detected throughout nascent heart parenchyma (Figures 6G, inset). Live born 3F-iPS demonstrated iPS contribution and engraftment throughout adult tissues with dark coat color visible on the white background (n=5; Figure 6H). Transgenic luciferase expression emanating from labeled iPS progeny upon *in vivo* imaging ranged from undetectable levels to a high degree of achieved chimerism. Chimeric offspring (n=5), including those with the highest contribution of iPS progeny (Figure 6I), demonstrated tumor-free assimilation throughout the 3 months of follow-up. This profile was independently verified by lack of tumor formation during 7.5 months of prospective follow-up upon subcutaneous injection of 500,000 3F-iPS into the flank of immunocompent hosts (n=6, data not shown). In line with non-disruptive integration, iPS chimera (n=5) exhibited vital signs, including average body weight, core temperature, heart and respiratory rates, that were indistinguishable from non-chimera counterparts (n=5; Table 1). Based on continuous electrocardiography, the chimeric cohort was devoid of ectopy, arrhythmias, or conduction blocks (Figure 6J). Comprehensive echocardiography analysis further demonstrated consistent cardiac structure between 3F-iPS chimera and non-chimera cohorts with similar measured values for aortic, pulmonary, and right outflow tract diameters, along with equivalent left atrium and left ventricular volumes (Table 1). Synchronized four-chamber function throughout systolic and diastolic cardiac cycles, indicating functional integration of 3F-iPS progeny into the adult organ, was also equivalent to non-chimera counterparts (n=5, Figure 6K and Table 1). Left ventricular functional performance of all 3F-iPS chimeras was essentially identical, according to measured fractional shortening and ejection fraction, compared to age and sex-matched normal controls (Table 1). Together, this evidence indicates a high proficiency for 3F-iPS progeny to contribute to normal heart formation, and sustain chimeric tissue without disruption to myocardial structure or function throughout prenatal to postnatal development. function as a blastomere, demonstrated by mosaic distribution of positive lacZ-expressing iPS progeny (Figure 6C and 6D). iPS-derived tissue populated the embryo (n=7) during development and contributed to all stages of cardiogenesis from primitive heart fields to

looped heart tubes corresponding to 8.0 to 9.5 dpc, respectively (Figures 6E–6G). By 9.5 dpc when the heart tube has fully looped to form distinct inflow and outflow tracts, iPS progeny was detected throughout nascent heart parenchyma (Figures 6G, inset). Live born 3F-iPS demonstrated iPS contribution and engraftment throughout adult tissues with dark coat color visible on the white background (n=5; Figure 6H). Transgenic luciferase expression emanating from labeled iPS progeny upon *in vivo* imaging ranged from undetectable levels to a high degree of achieved chimerism. Chimeric offspring (n=5), including those with the highest contribution of iPS progeny (Figure 6I), demonstrated tumor-free assimilation throughout the 3 months of follow-up. This profile was independently verified by lack of tumor formation during 7.5 months of prospective follow-up upon subcutaneous injection of 500,000 3F-iPS into the flank of immunocompent hosts (n=6, data not shown). In line with non-disruptive integration, iPS chimera (n=5) exhibited vital signs, including average body weight, core temperature, heart and respiratory rates, that were indistinguishable from non-chimera counterparts (n=5; Table 1). Based on continuous electrocardiography, the chimeric cohort was devoid of ectopy, arrhythmias, or conduction blocks (Figure 6J). Comprehensive echocardiography analysis further demonstrated consistent cardiac structure between 3F-iPS chimera and non-chimera cohorts with similar measured values for aortic, pulmonary, and right outflow tract diameters, along with equivalent left atrium and left ventricular volumes (Table 1). Synchronized four-chamber function throughout systolic and diastolic cardiac cycles, indicating functional integration of 3FiPS progeny into the adult organ, was also equivalent to non-chimera counterparts (n=5, Figure 6K and Table 1). Left ventricular functional performance of all 3F-iPS chimeras was essentially identical, according to measured fractional shortening and ejection fraction, compared to age and sex-matched normal controls (Table 1). Together, this evidence indicates a high proficiency for 3F-iPS progeny to contribute to normal heart formation, and sustain chimeric tissue without disruption to myocardial structure or function throughout prenatal to postnatal development.

Discussion

Nuclear reprogramming resets parental cell fate enabling derivation of pluripotent stem cells from somatic tissues. To date, evidence for iPS-based cardiogenesis has primarily been obtained with a quartet set of stemness factors that have utilized c-Myc or an equivalent transcription factor, Lin28, to generate isolated cardiac tissue *in vitro*.[13–17] Here, we demonstrate reproducible cardiogenic differentiation of iPS bioengineered independently of c-MYC throughout embryonic development and into adulthood.

In the absence of the pro-cardiogenic proto-oncogene, c-MYC, 3F-iPS clones reprogrammed ordinary tissue with “cross-species” human stemness factors, OCT4, SOX2, and KLF4, were qualified according to increasing levels of stringency for functional pluripotency from atavistic gene expression profiles to morula integration and *in utero* derivation of chimeric embryos. Reversal of the acquired pluripotent ground state was demonstrated within the embryoid body microenvironment to consistently, across distinct 3F-iPS clones, yield proficient cardiogenic progeny. Lineage specification *in vitro* allowed isolation of cardiomyocytes that inherited properties of functional excitation-contraction coupling. These were validated *in vivo* by sustained chimerism into adulthood that supported the high demands of normal heart performance. The feasibility of generating c-Myc-less iPS reprogramming, albeit from adult neuronal stem cells with murine orthologs, has recently produced progeny capable of differentiating into cardiac-like cells.[42] Although starting from alternative sources, i.e., adult stem cells versus the somatic tissue herein, these studies collectively support the notion that iPS generated independently of c-Myc are capable of cardiogenesis. Of note, the present study further demonstrates the functionality of derived cardiomyocytes from *in vitro* to *in vivo* model systems with gene expression, contractile

machinery, and regulation of membrane excitability generating synchronize calcium dynamics and coordinated mechanical contractions from chimeric tissues in embryos through adulthood. Thus, 3F-iPS biotechnology secures lineage-specific production of *bona fide* cardiac tissues utilizing a nuclear reprogramming approach that minimizes oncogenic exposure and fulfills, as demonstrated here, high-stringency criteria for derivation of functional cardiomyocytes.

In principle, reprogramming pluripotency without the oncogene c-Myc is a favorable strategy for iPS derivation given the reduction in dysregulated gene expression networks and tumorigenic load.25,26 Indeed 3F-iPS injected here into immunocompetent host did not produce dysregulated tumor growth in long-term follow-up. Moreover, 3F-iPS chimeras also did not demonstrate tumor formation and yet maintained a robust cardiogenic potential from differentiation to functional chimerism, independent of the pro-cardiogenic influence of c-Myc. However, this pleiotropic transcription factor is also a recognized dynamic regulator of the balance between growth and differentiation with ectopic transgene expression modulating lineage-specification.[43] A role for the proto-oncogene in the cardiac lineage was originally revealed in the setting of cardiac hypertrophy, where the c-Myc-dependent fetal gene profile is reactivated with expression of atrial genes and embryonic isoforms of contractile machinery in response to induction of immediate early genes (c-fos, c-myc, c-jun).[27] In fact, promiscuous c-Myc is required for embryonic development with cardiogenic disruption precipitating lethal embryonic dysregulation.44 This led to the observation that constitutive expression of c-Myc is sufficient to drive cardiac hyperplasia during development,45 and is responsible in part for adaptive compensation and survival benefit under cardiac stress in the adult.28,[29] While overexpression of c-Myc in the context of nuclear reprogramming has generated iPS with cardiogenic capacity,[13–17] c-Myc-less progeny here demonstrated comprehensive cardiogenic potential. The data suggest the dispensability of the pro-cardiogenic transcription factor during the reprogramming process, and establish the robustness of inherent cardiogenic differentiation networks in reprogrammed progeny.

Beyond surrogate markers of lineage differentiation, diploid aggregation with transplantation of bioengineered progenitors into a host embryonic environment provided a definitive screen to distinguish *de novo* cardiogenicity from the embryo into the adult. By non-coerced aggregation of pluripotent stem cells with early stage morulae, functional pluripotency is unequivocally demonstrated by successful incorporation of blastomere-like progenitors within the host embryo.[40] Here, the ability of 3F-iPS progeny to integrate into host embryos and recapitulate authentic cardiogenesis, indistinguishable from native tissue, was validated by normal electrical conduction patterns on surface electrocardiography, and proper cardiac structure and function according to trans-thoracic echocardiography demonstrated within healthy chimeric offspring. Indeed, engineered chimerism offers an unbiased model system to track developmental adequacy and provide a unique platform to determine the impact of stem cells on integrated physiology across lifespan.[40,46,47] By preventing the allogeneic incompatibility of post-natal transplantation, morula-derived iPS chimerism creates a genuine autologous niche for examining the ability of bioengineered progenitors to sustain structural and functional integrity and provide life-long adaptability to physiological demands. Thereby, the chimeric model system established here allowed *in vivo* validation of cardiogenic potential, and demonstrated the acquired ability of 3F-iPS to function interchangeably with native heart tissue, fulfilling criteria of *bona fide* cardiac progenitors.

In summary, iPS technology promises the next generation of cell-based biologics. With the prioritized goal of producing a somatic tissue source for reproducible tissue-specific differentiation, reprogramming strategies initially qualified according to functional

pluripotency and reduced tumorigenesis are here validated to produce *de novo* cardiogenic lineages. Reprogramming somatic tissue without transgenic c-MYC expression offers a reliable platform to ensure proficient iPS-derived cardiogenesis that achieves seamless integration and functional contribution to pre and postnatal cardiac performance.

Acknowledgments

We thank Lois Rowe for expert histological analysis.

Sources of Funding This work was supported by National Institutes of Health (R01HL083439, T32HL007111, R01HL085208, R56AI074363), American Heart Association, American Society for Clinical Pharmacology and Therapeutics, La Caixa Foundation Graduate Program, Marriott Individualized Medicine Program, Marriott Heart Disease Research Program, Gerstner Family Career Development Award in Individualized Medicine, and Mayo Clinic.

Non-standard abbreviations and acronyms

iPS	induced pluripotent stem cells
3F-iPS	three factor-induced pluripotent stem cells

References

1. Yamanaka S. A fresh look at iPS cells. Cell 2009;137:13–17. [PubMed: 19345179]
2. Hochedlinger K, Plath K. Epigenetic reprogramming and induced pluripotency. Development 2009;136:509–523. [PubMed: 19168672]
3. Nishikawa S, Goldstein RA, Nierras CR. The promise of human induced pluripotent stem cells for research and therapy. Nat Rev Mol Cell Biol 2008;9:725–729. [PubMed: 18698329]
4. Takahashi K, Okita K, Nakagawa M, Yamanaka S. Induction of pluripotent stem cells from mouse embryonic and adult fibroblast cultures by defined factors. Cell 2006;126:663–676. [PubMed: 16904174]
5. Markoulaki S, Hanna J, Beard C, Carey BW, Cheng AW, Lengner CJ, Dausman JA, Fu D, Gao Q, Wu S, Cassady JP, Jaenisch R. Transgenic mice with defined combinations of drug-inducible reprogramming factors. Nat Biotechnol 2009;27:169–171. [PubMed: 19151700]
6. Hanna J, Markoulaki S, Schorderet P, Carey BW, Beard C, Wernig M, Creyghton MP, Steine EJ, Cassady JP, Foreman R, Lengner CJ, Dausman JA, Jaenisch R. Direct reprogramming of terminally differentiated mature B lymphocytes to pluripotency. Cell 2008;133:250–264. [PubMed: 18423197]
7. Park I-H, Arora N, Huo H, Maherali N, Ahfeldt T, Shimamura A, Lensch MW, Cowan C, Hochedlinger K, Daley GQ. Disease-specific induced pluripotent stem cells. Cell 2008;134:877–886. [PubMed: 18691744]
8. Dimos JT, Rodolfa KT, Niakan KK, Weisenthal LM, Mitsumoto H, Chung W, Croft GF, Saphier G, Leibel R, Goland R, Wichterle H, Henderson CE, Eggan K. Induced pluripotent stem cells generated from patients with ALS can be differentiated into motor neurons. Science 2008;321:1218–1221. [PubMed: 18669821]
9. Yu J, Vodyanik MA, Smuga-Otto K, Antosiewicz-Bourget J, Frane JL, Tian S, Nie J, Jonsdottir GA, Ruotti V, Stewart R, Slukvin I, Thomson JA. Induced pluripotent stem cell lines derived from human somatic cells. Science 2007;318:1917–1920. [PubMed: 18029452]
10. Hanna J, Wernig M, Markoulaki S, Sun CW, Meissner A, Cassady JP, Beard C, Brambrink T, Wu LC, Townes TM, Jaenisch R. Treatment of sickle cell anemia mouse model with iPS cells generated from autologous skin. Science 2007;318:1920–1923. [PubMed: 18063756]
11. Wernig M, Zhao JP, Pruszak J, Hedlund E, Fu D, Soldner F, Broccoli V, Constantine-Paton M, Isacson O, Jaenisch R. Neurons derived from reprogrammed fibroblasts functionally integrate into the fetal brain and improve symptoms of rats with Parkinson's disease. Proc Natl Acad Sci USA 2008;105:5856–5861. [PubMed: 18391196]

12. Xu D, Alipio Z, Fink LM, Adcock DM, Yang J, Ward DC, Ma Y. Phenotypic correction of murine hemophilia A using an iPS cell-based therapy. Proc Natl Acad Sci USA 2009;106:808–813. [PubMed: 19139414]
13. Schenke-Layland K, Rhodes KE, Angelis E, Butylkova Y, Heydarkhan-Hagvall S, Gekas C, Zhang R, Goldhaber JI, Mikkola HK, Plath K, MacLellan WR. Reprogrammed mouse fibroblasts differentiate into cells of the cardiovascular and hematopoietic lineages. Stem Cells 2008;26:1537–1546. [PubMed: 18450826]
14. Mauritz C, Schwanke K, Reppel M, Neef S, Katsirntaki K, Maier LS, Nguemo F, Menke S, Haustein M, Hescheler J, Hasenfuss G, Martin U. Generation of functional murine cardiac myocytes from induced pluripotent stem cells. Circulation 2008;118:507–517. [PubMed: 18625890]
15. Narazaki G, Uosaki H, Teranishi Mm, Okita K, Kim B, Matsuoka S, Yamanaka S, Yamashita JK. Directed and systematic differentiation of cardiovascular cells from mouse induced pluripotent stem cells. Circulation 2008;118:498–506. [PubMed: 18625891]
16. Zhang J, Wilson G, Soerens A, Koonce C, Yu J, Palecek S, Thomson J, Kamp T. Functional cardiomyocytes derived from human induced pluripotent stem cells. Circ Res 2009;104:e30–41. [PubMed: 19213953]
17. Nelson TJ, Martinez-Fernandez A, Yamada S, Perez-Terzic C, Ikeda Y, Terzic A. Repair of acute myocardial infarction with human stemness factors induced pluirpotent stem cells. Circulation 2009;120:408–416. [PubMed: 19620500]
18. Nelson TJ, Behfar A, Terzic A. Stem cells: biologics for regeneration. Clin Pharmacol Ther 2008;84:620–623. [PubMed: 18701884]
19. Tanaka T, Tohyama S, Murata M, Nomura F, Kaneko T, Chen H, Hattori F, Egashira T, Seki T, Ohno Y, Koshimizu U, Yuasa S, Ogawa S, Yamanaka S, Yasuda K, Fukuda K. In vitro pharmacologic testing using human induced pluripotent stem cell-derived cardiomyocytes. Biochem Biophys Res Commun 2009;385:497–502. [PubMed: 19464263]
20. Stadtfeld M, Nagaya M, Utikal J, Weir G, Hochedlinger K. Induced pluripotent stem cells generated without viral integration. Science 2008;322:945–949. [PubMed: 18818365]
21. Okita K, Nakagawa M, Hyenjong H, Ichisaka T, Yamanaka S. Generation of mouse induced pluripotent stem cells without viral vectors. Science 2008;322:949–953. [PubMed: 18845712]
22. Woltjen K, Michael IP, Mohseni P, Desai R, Mileikovsky M, Hämäläinen R, Cowling R, Wang W, Liu P, Gertsenstein M, Kaji K, Sung HK, Nagy A. piggyBac transposition reprograms fibroblasts to induced pluripotent stem cells. Nature 2009;458:766–770. [PubMed: 19252478]
23. Yu J, Hu K, Smuga-Otto K, Tian S, Stewart R, Slukvin II, Thomson JA. Human Induced pluripotent stem cells free of vector and transgene sequences. Science 2009;324:797–801. [PubMed: 19325077]
24. Nelson TJ, Terzic A. Induced pluripotent stem cells: Reprogrammed without a trace. Regen Med 2009;4:333–335. [PubMed: 19438303]
25. Nakagawa M, Koyanagi M, Tanabe K, Takahashi K, Ichisaka T, Aoi T, Okita K, Mochiduki Y, Takizawa N, Yamanaka S. Generation of induced pluripotent stem cells without Myc from mouse and human fibroblasts. Nat Biotechnol 2008;26:101–106. [PubMed: 18059259]
26. Wernig M, Meissner A, Cassady JP, Jaenisch R. c-Myc is dispensable for direct reprogramming of mouse fibroblasts. Cell Stem Cell 2008;2:10–12. [PubMed: 18371415]
27. Izumo S, Nadal-Ginard B, Mahdavi V. Protooncogene induction and reprogramming of cardiac gene expression produced by pressure overload. Proc Natl Acad Sci USA 1988;85:339–343. [PubMed: 2963328]
28. Xiao G, Mao S, Baumgarten G, Serrano J, Jordan MC, Roos KP, Fishbein MC, MacLellan WR. Inducible activation of c-Myc in adult myocardium in vivo provokes cardiac myocyte hypertrophy and reactivation of DNA synthesis. Circ Res 2001;89:1122–1129. [PubMed: 11739276]
29. Zhong W, Mao S, Tobis S, Angelis E, Jordan MC, Roos KP, Fishbein MC, de Alborán IM, MacLellan WR. Hypertrophic growth in cardiac myocytes is mediated by Myc through a Cyclin D2-dependent pathway. EMBO J 2006;25:3869–3879. [PubMed: 16902412]
30. Amabile G, Meissner A. Induced pluripotent stem cells: current progress and potential for regenerative medicine. Trends Mol Med 2009;15:59–68. [PubMed: 19162546]

31. Nelson TJ, Martinez-Fernandez AJ, Yamada S, Mael AA, Terzic A, Ikeda Y. Induced pluripotent reprogramming from promiscuous human stemness-related factors. Clin Translation Sci 2009;2:118–126.
32. Guo W, Lasky JL, Chang CJ, Mosessian S, Lewis X, Xiao Y, Yeh JE, Chen JY, Iruela-Arispe ML, Varella-Garcia M, Wu H. Multi-genetic events collaboratively contribute to Pten-null leukaemia stem-cell formation. Nature 2008;453:529–533. [PubMed: 18463637]
33. Perez-Terzic C, Faustino RS, Boorsma BJ, Arrell DK, Niederländer NJ, Behfar A, Terzic A. Stem cells transform into a cardiac phenotype with remodeling of the nuclear transport machinery. Nat Clin Pract Cardiovasc Med 2007;4(Suppl 1):S68–76. [PubMed: 17230218]
34. Perez-Terzic C, Behfar A, Méry A, van Deursen JM, Terzic A, Pucéat M. Structural adaptation of the nuclear pore complex in stem cell-derived cardiomyocytes. Circ Res 2003;92:444–452. [PubMed: 12600892]
35. Behfar A, Zingman LV, Hodgson DM, Rauzier JM, Kane GC, Terzic A, Pucéat M. Stem cell differentiation requires a paracrine pathway in the heart. FASEB J 2002;16:1558–1566. [PubMed: 12374778]
36. Behfar A, Perez-Terzic C, Faustino RS, Arrell DK, Hodgson DM, Yamada S, Puceat M, Niederländer N, Alekseev AE, Zingman LV, Terzic A. Cardiopoietic programming of embryonic stem cells for tumor-free heart repair. J Exp Med 2007;204:405–420. [PubMed: 17283208]
37. Nelson TJ, Chiriac A, Faustino RS, Crespo-Diaz RJ, Behfar A, Terzic A. Lineage specification of Flk-1^{+} progenitors is associated with divergent Sox7 expression in cardiopoiesis. Differentiation 2009;77:248–255. [PubMed: 19272523]
38. Nelson TJ, Faustino RS, Chiriac A, Crespo-Diaz R, Behfar A, Terzic A. CXCR4^{+}/FLK-1^{+} biomarkers select a cardiopoietic lineage from embryonic stem cells. Stem Cells 2008;26:1464–1473. [PubMed: 18369102]
39. Hodgson DM, Behfar A, Zingman LV, Kane GC, Perez-Terzic C, Alekseev AE, Pucéat M, Terzic A. Stable benefit of embryonic stem cell therapy in myocardial infarction. Am J Physiol Heart Circ Physiol 2004;287:H471–479. [PubMed: 15277190]
40. Nelson TJ, Martinez-Fernandez A, Terzic A. KCNJ11 knockout morula reengineered by stem cell diploid aggregation. Phil Trans R Soc Lond B Biol Sci 2009;364:269–276. [PubMed: 18977736]
41. Yamada S, Nelson TJ, Crespo-Diaz RJ, Perez-Terzic C, Liu XK, Miki T, Seino S, Behfar A, Terzic A. Embryonic stem cell therapy of heart failure in genetic cardiomyopathy. Stem Cells 2008;26:2644–2653. [PubMed: 18669912]
42. Kim JB, Sebastiano V, Wu G, Araúzo-Bravo MJ, Sasse P, Gentile L, Ko K, Ruau D, Ehrich M, van den Boom D, Meyer J, Hübner K, Bernemann C, Ortmeier C, Zenke M, Fleischmann BK, Zaehres H, Schöler HR. Oct4-induced pluripotency in adult neural stem cells. Cell 2009;136:411–419. [PubMed: 19203577]
43. Guo Y, Niu C, Breslin P, Tang M, Zhang S, Wei W, Kini AR, Paner GP, Alkan S, Morris SW, Diaz M, Stiff PJ, Zhang J. c-Myc-mediated control of cell fate in megakaryocyte-erythrocyte progenitors. Blood. DOI 10.1182/blood-2009-01-197947.
44. Baudino TA, McKay C, Pendeville-Samain H, Nilsson JA, Maclean KH, White EL, Davis AC, Ihle JN, Cleveland JL. c-Myc is essential for vasculogenesis and angiogenesis during development and tumor progression. Genes Dev 2002;16:2530–2543. [PubMed: 12368264]
45. Jackson T, Allard MF, Sreenan CM, Doss LK, Bishop SP, Swain JL. The c-myc proto-oncogene regulates cardiac development in transgenic mice. Mol Cell Biol 1990;10:3709–3716. [PubMed: 1694017]
46. Yamada S, Nelson TJ, Behfar A, Crespo-Diaz RJ, Fraidenraich D, Terzic A. Stem cell transplant into pre-implantation embryo yields myocardial infarction-resistant adult phenotype. Stem Cells 2009;27:1697–1705. [PubMed: 19544428]
47. Stillwell E, Vitale J, Zhao Q, Beck A, Schneider J, Khadim F, Elson G, Altaf A, Yehia G, Dong J-H, Liu J, Mark W, Bhaumik M, Grange R, Fraidenraich D. Blastocyst injection of wild type embryonic stem cells induces global corrections in mdx mice. PLos ONE 2009;4:e4759. [PubMed: 19277212]

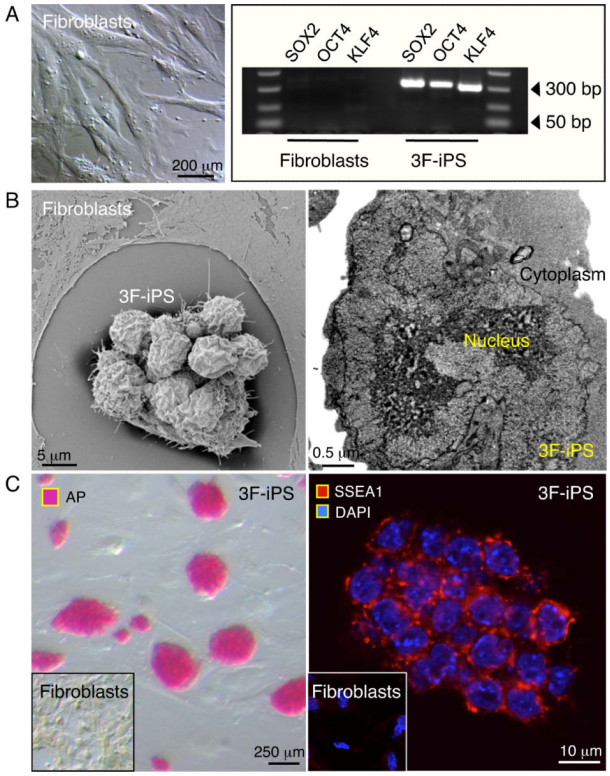

Figure 1.

Bioengineered pluripotency in the absence of c-MYC transgene. A, Mouse embryonic fibroblasts (left) were transduced with three HIV-derived lentiviruses containing human genes SOX2, OCT4 and KLF4. Genomic integration of viral constructs was detected in transduced progeny but not in parental fibroblast (right). B, Within three weeks, expression of the gene triad (3F) induced a dramatic change from flat fusiform fibroblasts to a round and compact embryonic-stem-cell-like morphology (left) with reduced cytoplasm (right). C, Reprogrammed cells acquired pluripotency markers alkaline phosphatase (AP; left) and SSEA-1 (right), absent from parental fibroblasts (inset).

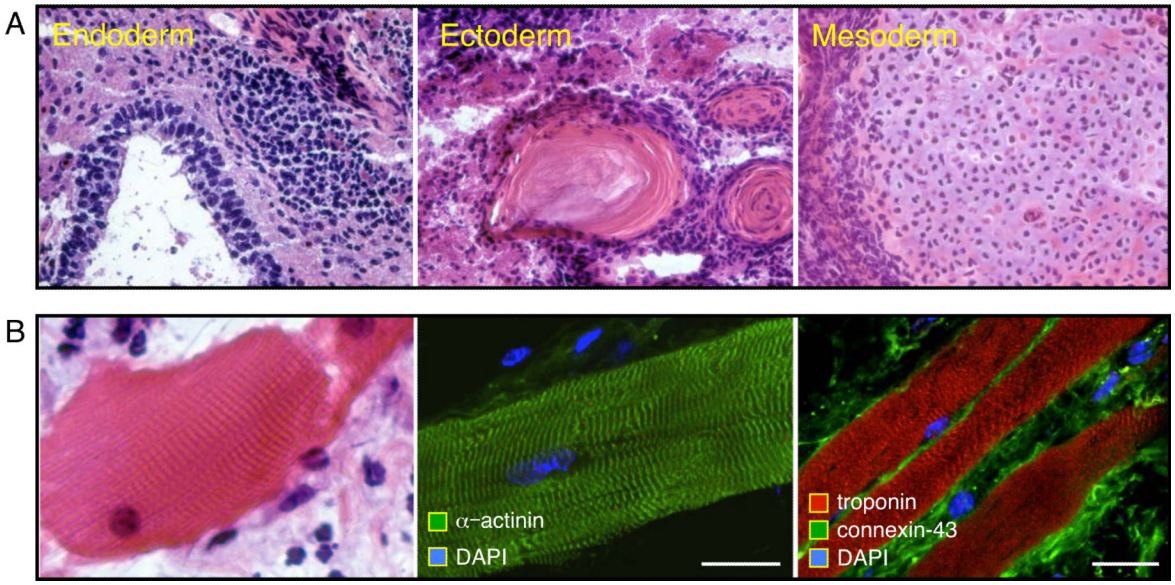

Figure 2.

Validated pluripotency of iPS according to *in vivo* differentiation. A, Fulfilling increasing levels of pluripotent stringency, 3F-iPS generated teratoma when injected subcutaneously into immunodeficient host. Tissues from the three germinal layers were identified by hematoxylin-eosin staining (40x magnification) represented by glandular epithelium (endoderm), keratinized epidermal ectoderm (ectoderm) and connective tissue (mesoderm). B, Cardiac tissue was found in teratomas derived from 3F-iPS as characterized by hematoxylin-eosin stained striations (left) and immunostaining for cardiac proteins α-actinin (middle), and troponin-I with connexin 43 (right). bar 10 μm. DAPI: 4,6'-diamidino-2-phenylindole.

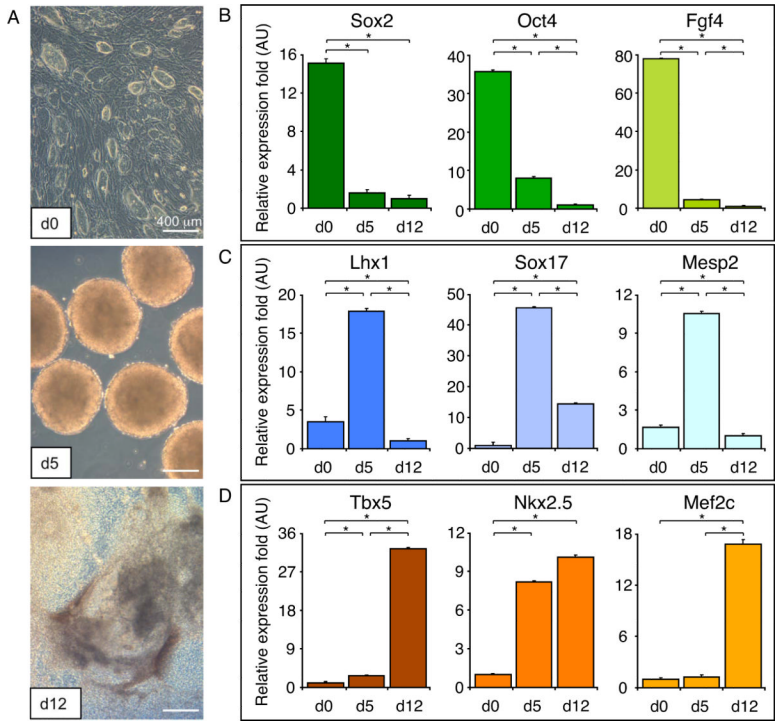

Figure 3.

Kinetics of *in vitro* lineage derivation from iPS. 3F-iPS were differentiated using the hanging drop method followed by expansion of progeny on gelatinized plates. A, Cells were sampled from undifferentiated cultures at day 0 (top), floating embryoid bodies at day 5 (middle) and differentiating cultures at day 12 (bottom) for gene expression analysis. B, Pluripotency genes Sox2, Oct4 and Fgf4 immediately downregulated with initiation of differentiation. C, Gastrulation markers peaked at day 5, coinciding with three germ layer formation in embryoid bodies. D, Upregulation of cardiac transcription factors Tbx5, Nkx2.5 and Mef2c was observed at day 12 indicating that 3F-iPS are able to produce cardiac progenitors. *p<0.05

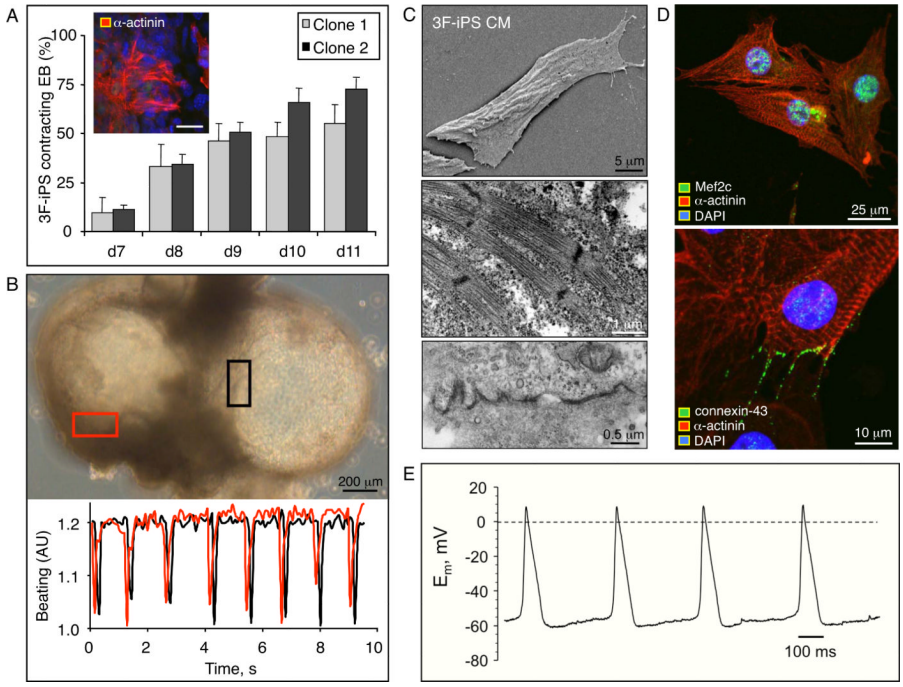

Figure 4.

Functional cardiogenesis derived from 3F-iPS. A, Derived from two independently isolated clones, embryoid bodies (EB) increasingly demonstrated beating areas between day 7 and 11 of differentiation. The presence of area actively contracting coincided with positive immunostaining for cardiac protein α-actinin (inset, bar 10 μm). B, Synchronized contractile activity (rectangles; top) was detected within adjacent EB (bottom). C, Electron microscopy of 3F-iPS derived cardiomyocytes (CM) revealed morphological changes from compacted colonies to rod-shaped cardiomyocyte-like cells (top). High density contractile proteins were found in organizing sarcomeres (middle) as well as gap junction structures between adjacent cells (bottom). D, Immunostaining demonstrated presence of contractile protein alpha actinin in combination with cardiac transcription factor Mef2c (top), and gap junction-protein connexin 43 (bottom). E, Action potentials were recorded in beating cells using patch clamp in the current clamp mode. DAPI: 4,6'-diamidino-2-phenylindole.

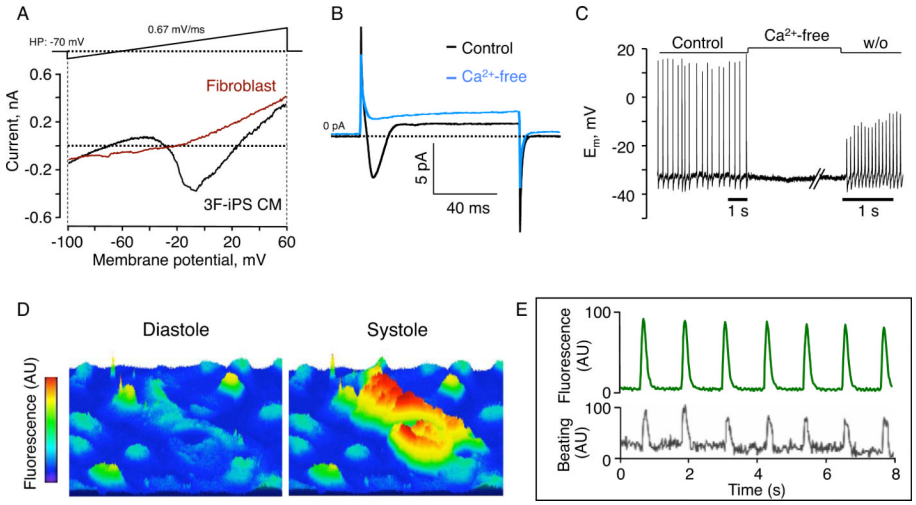

Figure 5.

Calcium-dependent excitation-contraction coupling in 3F-iPS-derived cardiomyocytes. A, An inward current was detected in iPS-derived cardiomyocytes (3F-iPS CM, black line) absent from parental fibroblasts (red line). B, Reversal of extracellular calcium suppressed inward current. C, Spontaneous action potentials were reversibly arrested in zero calcium milieu. D, Fluo-4AM labeled iPS-derived cells demonstrated fluorescent dynamics consistent with calcium transients. E, Rhythmic calcium transients coincided with cell contractions.

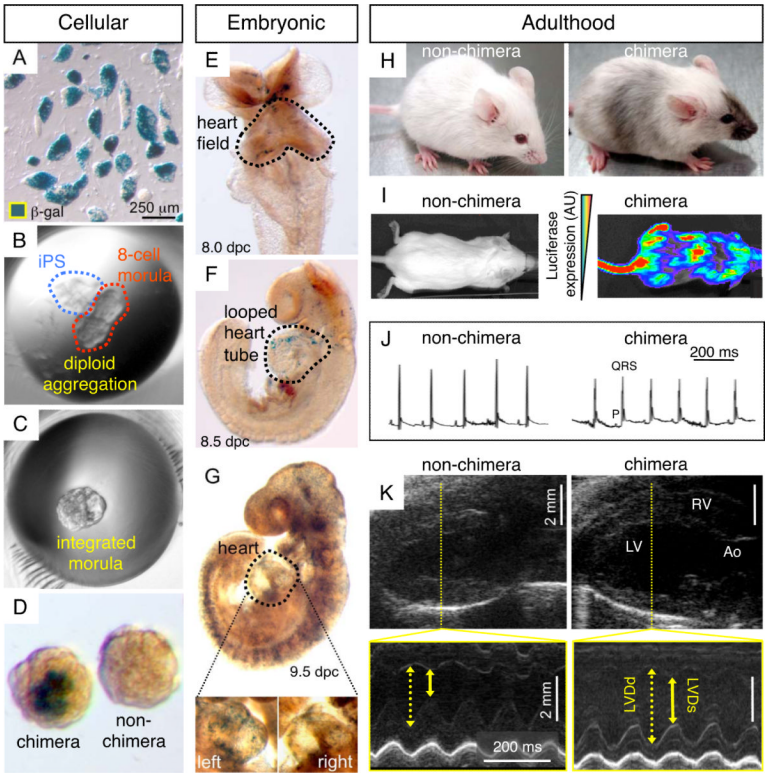

Figure 6.

iPS bioengineered cardiac chimerism contributes to sustained heart function throughout development and lifespan. (A–B) LacZ labeled-iPS coincubated with diploid embryos. (C–D) Chimeras revealed the ability of 3F-iPS to integrate into host morulae. (E–G) Presence of iPS was sustained throughout embryonic development as shown for 8.0 through 9.5 dpc contributing to cardiac inflow and outflow tracts (G, inset). H, Other than mosaic coat color, adult chimeras were physically indistinguishable from non-chimeric littermates. I, Increasing levels of chimeric expressed luciferase distributed within tissues were detected according to molecular imaging with iPS-derived progeny. J, Cardiac electrocardiography was equivalent between non-chimera and chimera. K, Cardiac echocardiography demonstrated normal structure of heart, valves, and great-vessels with equivalent systolic and diastolic function between non-chimera and chimera. Ao: aorta, LV: left ventricle; LVDd: left ventricular diastolic diameter, LVDs: left ventricular systolic diameter, RV: right ventricle. bar 2 mm.

Table 1

Cardiovascular comparison between non-chimera and 3F-iPS chimeric cohorts.

	Non-chimera	Chimera	p
Cohort, n	5	5	
Vital signs			
Body weight, g	33.8±1.0	36.2±2.1	0.25
Body core temperature, °C	35.2± 0.8	35.8±0.6	0.46
Respiration rate, /min	117±3	112±2	0.34
Heart rate, beats/min	469±10	455±9	0.29
Cardiovascular structure			
Ascending aorta, mm	1.68±1.09	1.58±0.04	0.35
Main pulmonary artery, mm	1.80±0.14	1.81±0.14	0.75
Right ventricular outflow tract, mm	1.32±0.18	1.31±0.19	0.99
Left atrium, mm	1.79±0.13	2.04±0.19	0.35
LVDd/BW, mm/g	0.106±0.01	0.113±0.01	0.60
Left ventricular end-diastolic volume, μL	59.2±3.3	61.5±6.3	0.92
Left wall thickness (septum plus posterior wall), mm	1.43±0.05	1.56±0.08	0.25
Left ventricle/body weight, mg/g	2.52±0.24	3.22±0.30	0.12
Cardiac function			
Fractional shortening, %	46.6±2.8	45.4±3.1	0.75
Ejection fraction, %	61.7±3.9	63.6±1.8	0.92

LVDd, left ventricular diastolic diameter. BW, body weight.